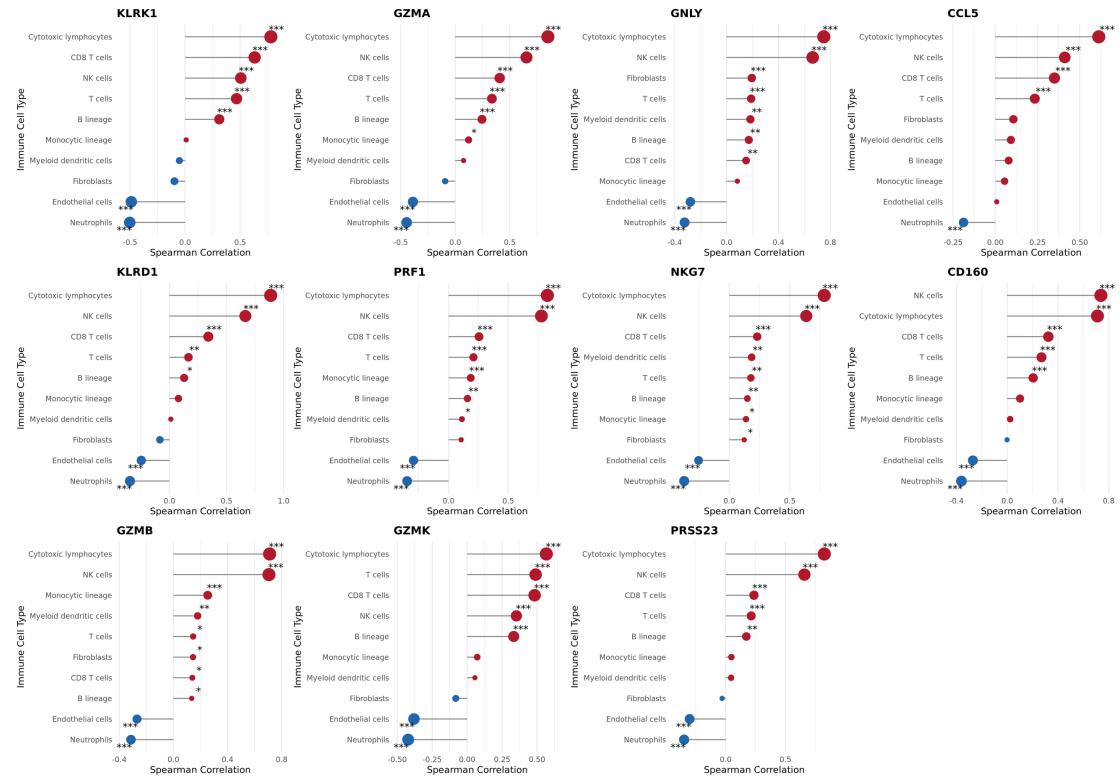
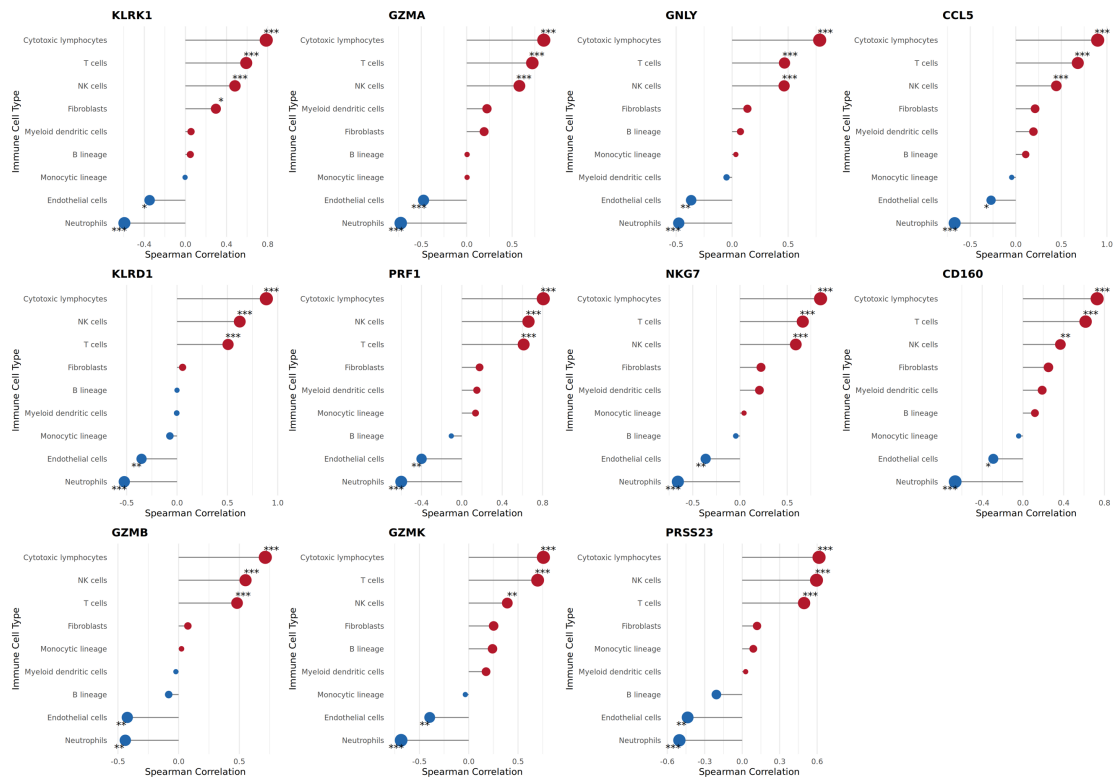


Supplementary Figure S1. Pre-processing quality control steps for SLE (GSE45291) and CAD (GSE61145) transcriptome sequencing datasets. A Principal component analysis (PCA) of SLE samples, demonstrating distinct clustering patterns between control (blue) and SLE (red) groups with 95% confidence ellipses; B PCA visualization for comparison between CAD datasets before (left) and after (right) ComBat batch effect correction, highlighting significant reduction of technical artifacts; C Expression density distributions are shown in SLE and CAD, with curves indicating expression frequency distributions across control (blue) and disease (red)

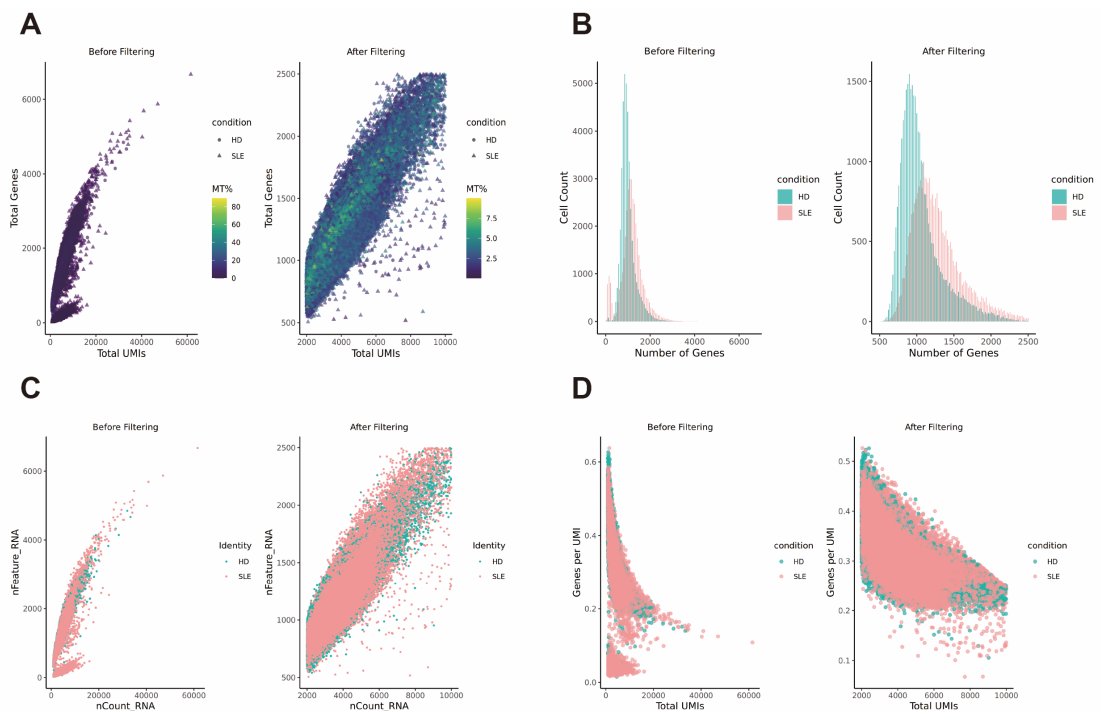
groups. D Sample-wise expression distributions displayed as heatmaps reveal gene expression homogeneity across individual disease samples and (SLE or CAD) control samples.



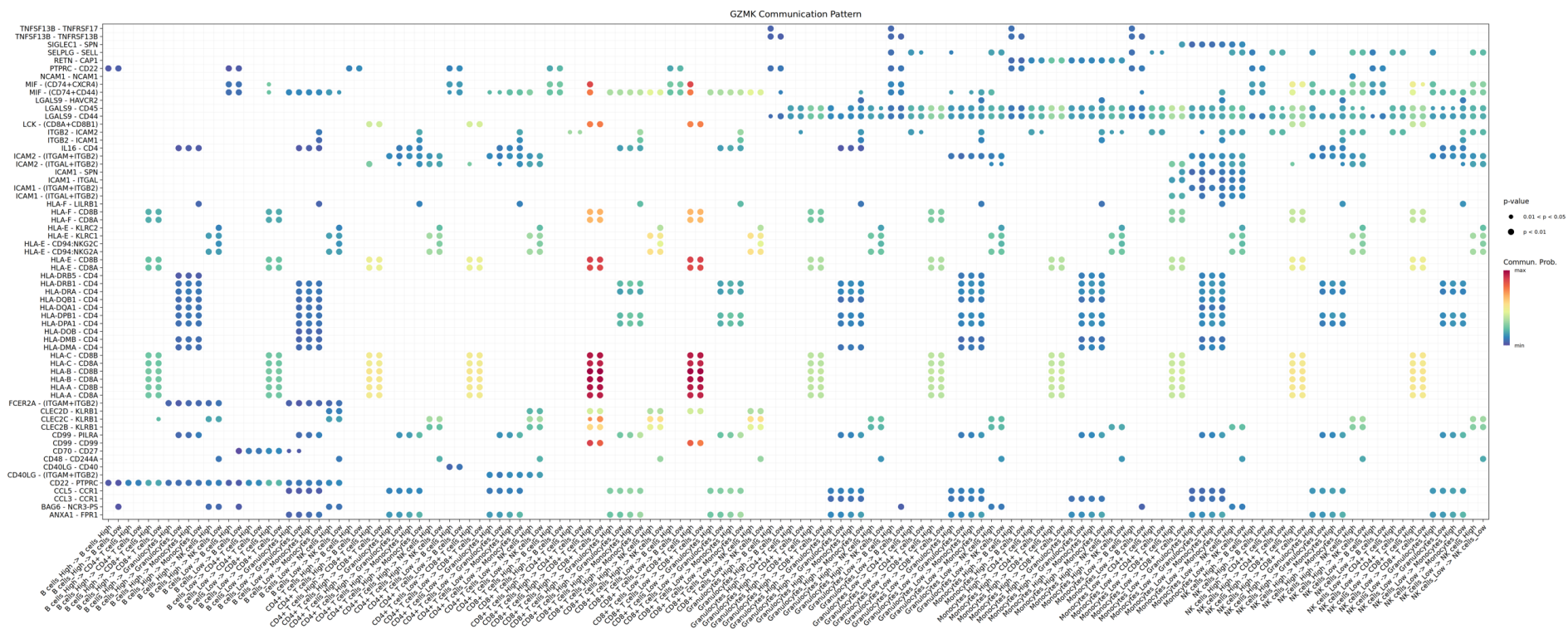
Supplementary Figure S2. Lollipop plot showing the correlation between the 11 genes with immune cells in SLE (GSE45291 dataset). The 11 genes include KLRK1, GZMA, GNL1, CCL5, KLRD1, PRF1, NKG7, CD160, GZMB, GZMK, and PRSS23. Immune cell types include cytotoxic lymphocytes, NK cells, CD8 T cells, T cells, B lineage, Monocytic lineage, Myeloid dendritic cells, Fibroblasts, Endothelial cells and Neutrophils. * $p < 0.05$; ** $p < 0.01$; *** $p < 0.001$.



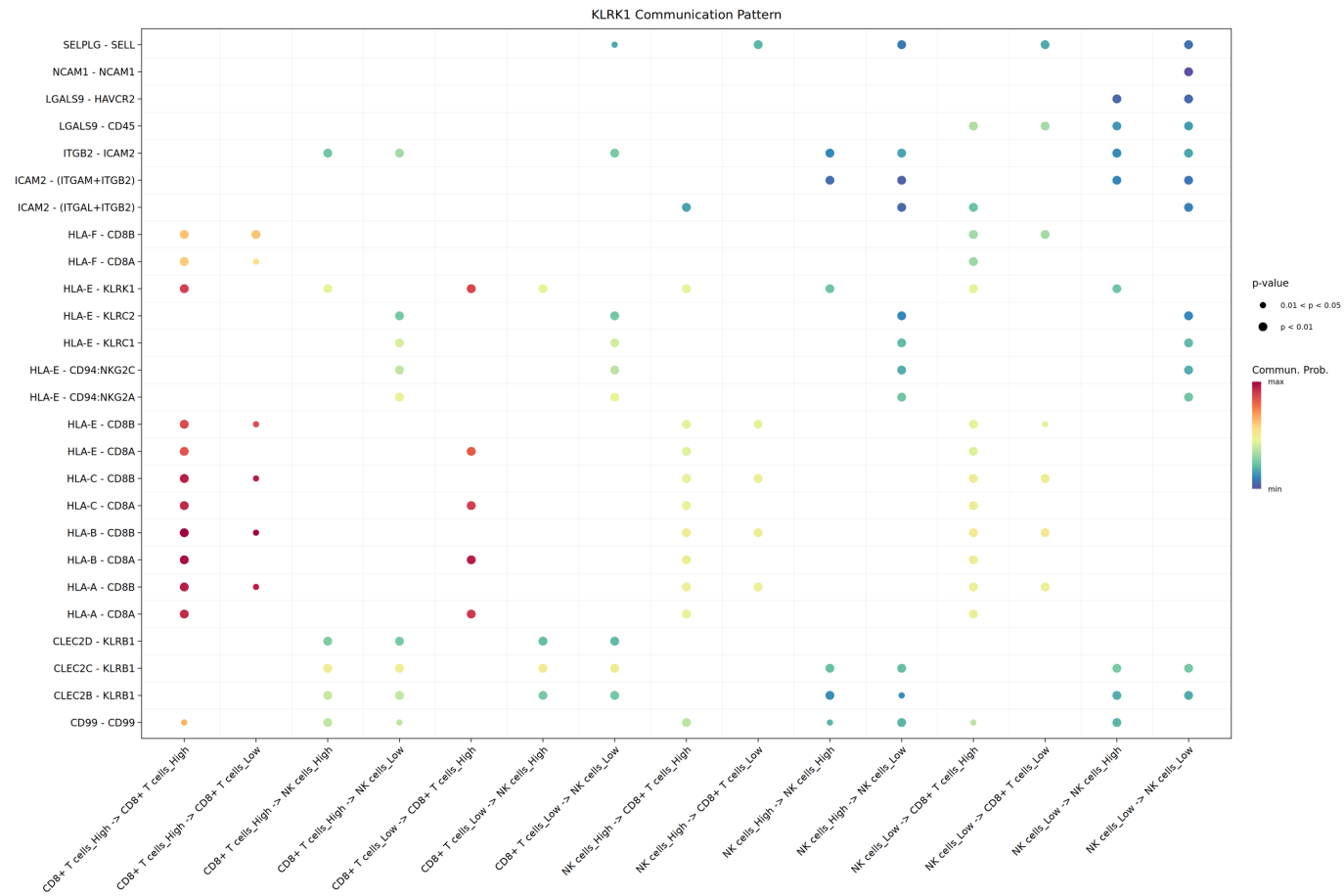
Supplementary Figure S3. Lollipop plot showing the correlation between the 11 genes with immune cells in CAD (GSE61145 dataset). The 11 genes include KLRK1, GZMA, GNLY, CCL5, KLRD1, PRF1, NKG7, CD160, GZMB, GZMK, and PRSS23. Immune cell types include cytotoxic lymphocytes, NK cells, T cells, B lineage, Monocytic lineage, Myeloid dendritic cells, Fibroblasts, Endothelial cells and Neutrophils. * $p < 0.05$; ** $p < 0.01$; *** $p < 0.001$.



Supplementary Figure S4. Quality control filtering of single-cell RNA sequencing data (GSE135779) from SLE. A. Scatter plots contrasting unfiltered (left) and filtered (right) data through the relationship between total detected genes (nGenes) and transcript counts (nUMIs), with point colors indicating mitochondrial read percentage (MT%) and shapes distinguishing healthy donor (HD, circles) and SLE (triangles) samples; B. Gene count distributions before (left) and after (after) filtration as histograms, with representing HD (blue) and SLE (red) populations; C. Scatter plots demonstrating the correlation between RNA feature counts and total RNA counts across filtration stages; D. Scatter plots visualizing gene detection efficiency via genes-per-UMI versus nUMIs relationships



Supplementary Figure S5. GZMK-mediated intercellular communication network. This dot plot visualizes the ligand-receptor interaction patterns mediated by GZMK across different cell types or conditions. Each dot represents a specific interaction pair, with the vertical axis indicating ligand identity and the horizontal axis denoting receptor or target cell categories. Dot color corresponds to communication probability, as shown in the gradient scale from blue (low probability) to red (high probability), while dot size reflects the statistical significance ($-\log_{10}$ transformed p-value) of each interaction.



Supplementary Figure S6. KLRK1-mediated intercellular communication network. This dot plot visualizes the ligand-receptor interaction patterns mediated by KLRK1 across different cell types or conditions. Each dot represents a specific interaction pair, with the vertical axis indicating ligand identity and the

horizontal axis denoting receptor or target cell categories. Dot color corresponds to communication probability, as shown in the gradient scale from blue (low probability) to red (high probability), while dot size reflects the statistical significance ($-\log_{10}$ transformed p-value) of each interaction.